Nanoscale

RSC Publishing

COMMUNICATION

Optical imaging of non-fluorescent nanodiamonds in live cells using transient absorption microscopy†

Cite this: *Nanoscale*, 2013, **5**, 4701

Received 17th January 2013
Accepted 4th April 2013

DOI: 10.1039/c3nr00308f

www.rsc.org/nanoscale

Tao Chen,‡[a] Feng Lu,‡[b] Aaron M. Streets,[a] Peng Fei,[a] Junmin Quan[b] and Yanyi Huang*[a]

We directly observe non-fluorescent nanodiamonds in living cells using transient absorption microscopy. This label-free technology provides a novel modality to study the dynamic behavior of nanodiamonds inside the cells with intrinsic three-dimensional imaging capability. We apply this method to capture the cellular uptake of nanodiamonds under various conditions, confirming the endocytosis mechanism.

Optical probes for live cell imaging are valuable tools in biomedical research. They illuminate important interesting biochemical processes inside cells. The inside of a living cell, however, is a rather complex biochemical environment, making it difficult to choose suitable probes that are both highly specific and biochemically inert. High contrast is also a key consideration for detection and visualization of probes. Genetically encoded fluorescent proteins and small-molecule fluorophores have long been used as imaging probes for their high chemical specificity.[1] In addition, numerous types of nanoparticles, including quantum dots, carbon nanotubes, and metallic nanorods, have been developed as optical imaging probes.[2–4] These nanoparticles, most of which can emit light, are becoming more widely used for cell studies because of their high quantum yield and chemical stability.[5] Some nanoparticle probes are intrinsically fluorescent, and others can be conjugated with functional molecules for fluorescence detection through surface modification. In addition to functioning as probes, many nanoparticles can also act as carriers, which bring other molecules, like proteins or drugs, into live cells.[6–9]

Among carbon nanomaterials[10–16] which are chemically inert and uniquely stable in live cells, nanodiamonds (NDs) show the least cytotoxicity. For this reason, nanodiamonds have been increasingly used for live cell applications. Ref. 17 reviews many of such applications including drug and small molecule delivery, as well as scaffolding for tissue engineering.

These nanoscale diamond crystals, with a typical diameter of around 4–5 nm, can be produced by detonation,[18] high-temperature and pressure synthesis,[19] or chemical vapor deposition.[20] The surface of NDs consists of a layer of sp^2 type C–C bonds, allowing chemical modifications such as hydroxylation, carboxylation, amination, and esterification.[21–24] Meanwhile, the inner diamond core, mainly sp^3 type C–C bonds, is completely inert under cellular environment. The ability to visualize NDs and their translocation dynamics within live cells is crucial to the understanding of cellular uptake mechanisms. In their raw form NDs are typically not photoluminescent. These raw particles can be made fluorescent by introduction of a negatively charged nitrogen-vacancy center (NV^- center). A NV^- center is a negatively charged nitrogen-vacancy pair inside the particle. Emission becomes stronger when there are more NV^- centers in a particle. The most widely used method to fabricate fluorescent NDs (fNDs) is high-energy particle irradiation or through high-pressure-high-temperature synthesis,[19,25] which require sophisticated experimental setups that are not easily accessible in most laboratories. Although fNDs exhibit great fluorescent quantum yield,[26] their adoption in biological research has been hindered by these complicated fabrication processes.

Here we present a new method using transient absorption microscopy (TAM) to directly observe raw NDs in live cells. Transient absorption (TA) is the secondary absorption of a photon through an electronic transition after a primary absorption event (Fig. 1a). This secondary absorption can only happen within the lifetime of the original excited state. When used as a contrast mechanism in microscopy, TA is a promising tool to perform label-free imaging of chromophores and nanoparticles in live cells and animals with a resolution close to

[a]*Biodynamic Optical Imaging Center (BIOPIC), College of Engineering, Peking University, Beijing, China. E-mail: yanyi@pku.edu.cn; Fax: +86-010-62758323; Tel: +86-010-62744058*

[b]*School of Chemical Biology and Biotechnology, Peking University Shenzhen Graduate School, Shenzhen, China*

† Electronic supplementary information (ESI) available. See DOI: 10.1039/c3nr00308f

‡ These authors contributed equally.

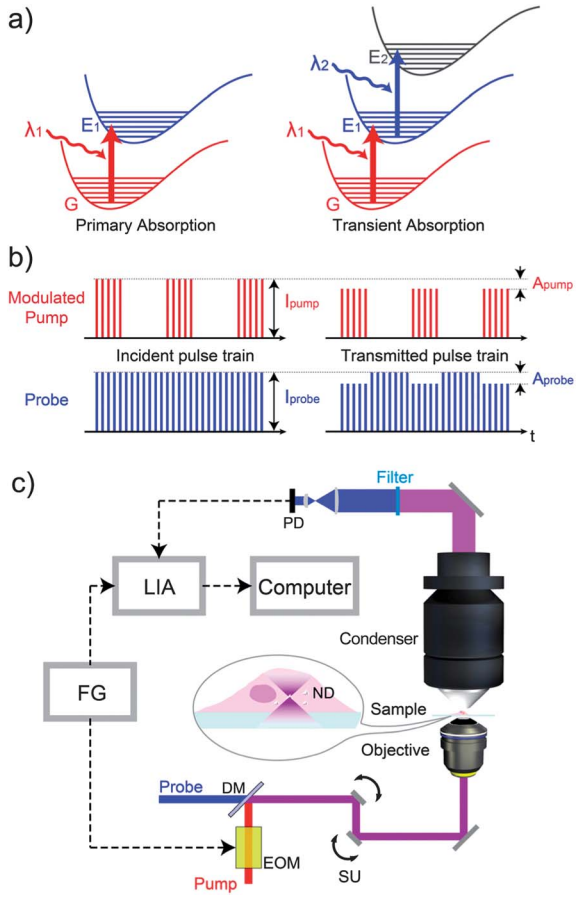

Fig. 1 Schematic of transient absorption: principle, method, and setup. (a) Primary and transient absorption; (b) pump probe modulation scheme. The pump beam (λ_1) was modulated at ~10 MHz causing the probe beam (λ_2) to experience a loss at the pump's modulation frequency; (c) a schematic of the excitation and collection setup. Pump (1064 nm) and probe beams are overlapped in space. After interacting with the sample, the probe beam was resized by a telescope and detected by a photodiode. The modulated signal is sent into a lock-in amplifier (LIA) and then to the computer for image reconstruction. EOM: electro optical modulator; DM: dichroic mirror; PD: photo-diode; SU: scanning unit; FG: function generator.

the optical diffraction limit.[27–29] Nanotubes have been shown to have strong TA signals, providing a new modality for bioimaging.[29] We found that NDs also possess a strong TA signal. This signal has intrinsic 3D sectioning capability, and is suitable for dynamic observation. Using transient absorption microscopy, we have investigated the interactions between NDs and live mammalian cells, including the process and mechanism of cell uptake and its environment dependent efficiency. We thus demonstrate that TA provides excellent contrast for imaging NDs in live cells.

We imaged NDs with TA by exciting the particles with a pump beam, and measuring the intensity suppression of a probe beam. In order to detect this intensity suppression, an electro-optical modulator (EOM) was used to modulate the pump beam (1064 nm) at a frequency of ~10 MHz, which was far from the center of the frequency spectrum of laser noise. Modulated intensity suppression of the probe beam was then demodulated and amplified by a lock-in amplifier (Fig. 1b and c).

The raw ND colloid was carboxylated under strong oxidizing conditions as previously reported[30] to create the hydrophilic particles and minimize colloidal aggregation in the suspension formation in aqueous buffers. After carboxylation, the ND suspension became more opaque and the color lightened (Fig. S1†). To further prevent ND aggregation (Fig. 2a and b) long-time (>5 hours) sonication and filtering are needed for generating a stable suspension before adding the NDs to the cell culture medium for uptake.

The TAM system has two laser beams, pump and probe, that are collinearly introduced into the microscope. This system is also capable of acquiring stimulated Raman scattering (SRS) images.[31] SRS microscopy offers the ability to detect many chemical species without labelling. NDs, as any other chemical species, have characteristic Raman signatures. To differentiate the TA signal from SRS, we first compared the signal strength generated from the ND suspension with the SRS signal of C–H stretching of CH_2 groups of tristearin. The strong signal at 2845 cm^{-1} has been widely applied for observing the lipid contents inside live cells. Compared with this signal, the intensity of Raman peaks of NDs is about one order of magnitude lower than that of tristearin (Fig. 2b), indicating that the SRS signal of NDs will present minimal background. Stimulated Emission[32] does not contribute to the background signal because the intrinsic phase is opposite to TA and SRS (ESI Fig. S10†).

Transient absorption, however, offers a much stronger signal, comparable with SRS of pure tristearin (Fig. 2b). It is not surprising that TA has a better signal strength than SRS because it is generated from the electronic transition, which has a much larger absorption cross-section (typically 10^{-17} to 10^{-16} cm^2)[33,34] compared with Raman scattering (typically ~10^{-30} and ~10^{-20} cm^2 for specific molecules).[35,36] The signal strength is sufficient for fast (2 μs per pixel) cell imaging, allowing one to observe the

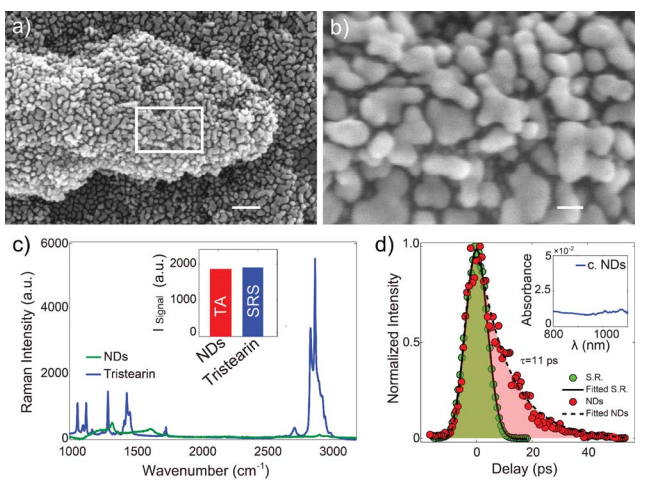

Fig. 2 Characterization of nanodiamonds. (a and b) Scanning electron microscope images of NDs dispensed on a silicon wafer. Scale bars are 100 nm in (a) and 20 nm in (b); (c) spontaneous Raman spectra of tristearin and NDs. The inset shows the comparison between NDs' TA signal and tristearin's SRS signal. (d) The temporal characteristics of NDs' TA. Green circles show the system response to pump–probe pulses correlation. Red circles show the intensity-delay dependence of the TA signal. The inset shows the absorption spectrum of carboxylated NDs from 800 to 1100 nm. c. NDs: carboxylated NDs.

dynamic behaviors of NDs in live cells. TA shows little harm to cells since both pump and probe beams are near-infrared and cells do not absorb much light at these wavelengths. The total irradiation power of 60 mW is safe for long-term observation of cells. For short-term experiments, up to 140 mW was also tolerable (Fig. S2–S6†). Small particles can be visualized by raising the excitation power without noticeable photodamage to the cells.

Transient absorption has characteristic dynamics that can be revealed by the time-delay pump–probe measurements. The delay time between the probe and pump beams affects the intensity of TA, as shown in Fig. 2c. The intensity decay can be deconvoluted using the system response (S.R.), giving a single exponential decay with a lifetime of 11 ps (Fig. 2d). The absorption of NDs has weak wavelength dependence (Fig. 2d inset), hence we can choose appropriate wavelengths to avoid strong ground state absorption or strong Raman resonance in the specimen.

After incubating the cells with ND suspension for 8 h, we can clearly observe the NDs in the cytoplasm of cells using TAM, as shown in Fig. 3a. To validate the cell uptake of NDs, we also stained the cell with FM4-64, a widely used membrane-selective amphiphilic styryl dye[37,38] to monitor endocytosis and vesicle trafficking in live cells (Fig. 3b). Fluorescence labeled vesicles inside the cell partly co-localized with NDs, indicating that the NDs are most likely transported into the cells through the endocytosis process, as has been observed by TEM.[30]

The decay dynamics of TA of NDs provides an excellent way to differentiate the signal from SRS. We chose the pump–probe combination at 1064/817 nm, which also fits the Raman scattering band of lipid C–H stretching. When the delay was set to zero (Fig. 3c), we could observe the bright dots, indicating the locations of NDs, as well as the smeared faint signal from lipid-rich sub-cellular organelles in live cells, outlining the cells. The nuclei can also be identified from the images since the cytoplasm is clearly brighter, reflecting the absence of lipid-rich contents in the nuclei. As the delay between the pump and the probe was tuned from zero, the SRS signal disappeared while the TA signal persisted (Fig. 3d) with decreased intensity. This time-delay method is an effective way to exclude the signal crosstalk from SRS. Another way to eliminate the SRS background is to set the pump–probe frequency difference in the silent region, a spectral range with typically no Raman peaks to suppress the SRS background. The advantage of the latter approach is that a delay time of zero can be used without sacrificing the TA signal intensity. The TA not only offers a strong signal for observing the raw NDs, but also eliminates the notorious autofluorescence background from the live cells.

The dynamic process of cell uptake of NDs was visualized by time-lapse TA imaging of single NDs entering the cells. The three dimensional snapshots of the high-resolution time-lapse images (Fig. 4a) show that two single ND particles were initially adsorbed to the cell membrane, dwelled for a short period of time (~10 min) and then quickly entered the cell. The intensity change at t_1 and t_2 indicated the times at which each particle entered the cell. We picked the probe wavelength at 808 nm for this observation because it also fits the SRS band of C–H stretching from CH_3, contributed mostly from protein contents

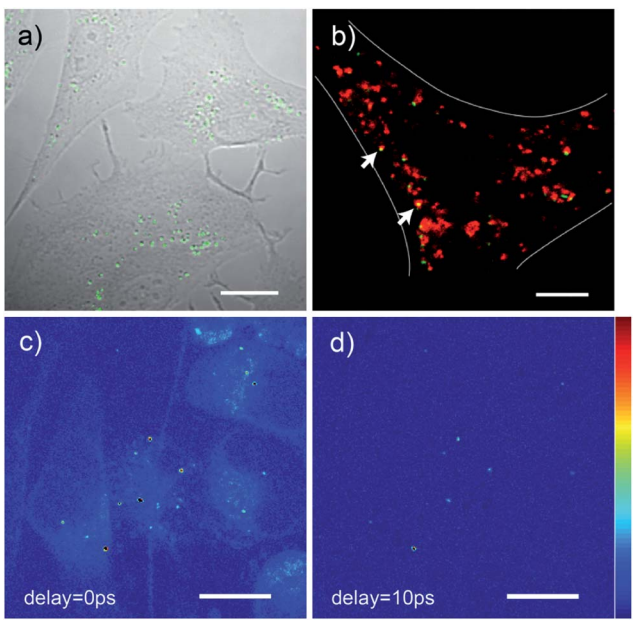

Fig. 3 Transient absorption images of NDs in NIH-3T3 cells. (a) Merged image of NDs' TAM (green) and transmitted bright field (gray) signals; (b) merged image of NDs' TAM (green) and FM4-64 confocal fluorescence (red) signals. White arrows indicate a few co-localizations of vesicles and NDs; (c and d) temporal property of NDs' TAM images in live cells. Both images were acquired in the lipid band. A faint lipid signal from cytoplasm could be seen in (c) but not in (d).

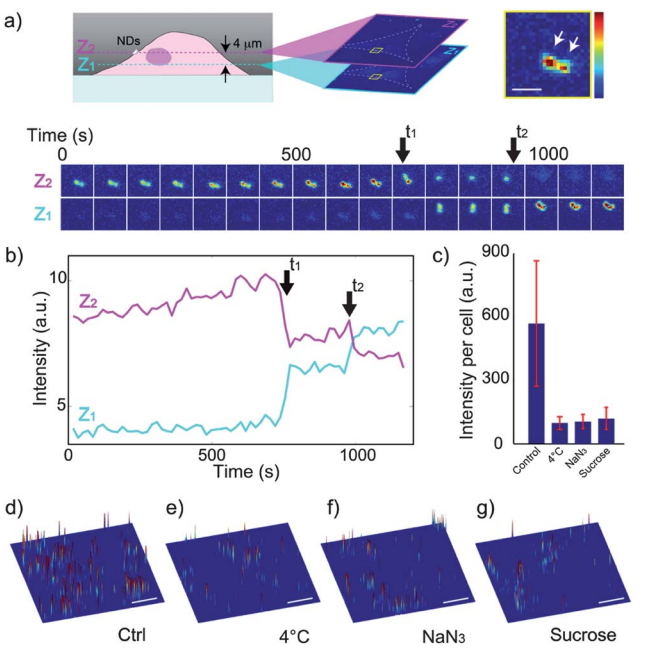

Fig. 4 Dynamic cell uptake of NDs. (a) A series of TAM images at two different focal planes. Z_2 contains part of the cell membrane and Z_1 is inside the cell. Two ND particles are indicated using arrows, the scale bar is 2 mm; (b) the evolution of TAM intensity at two focal planes; (c) a comparison of uptake efficiency under different culture conditions; (d–g) images of ND uptake under each culture condition. All scale bars are 20 mm.

in living cells, and provides a weak background of cell shape. The intensity of SRS is much weaker than NDs' TA signal, and therefore did not affect the observation. Fig. 4b shows the signal intensity captured at two different focal planes. At t_1, the intensity of focal plane Z_2 dropped and that of focal plane Z_1 increased, indicating that the first ND had been transported into the cell. At t_2, the second ND entered the cell. Considering the time resolution of our experiment, the actual uptake process could be finished within 30 s. TA of NDs was very stable, showing no photodamage or signal degradation during the whole acquisition of ~1 h.

In addition to the normal culture conditions, we tested the cell uptake efficiency under three other conditions (Fig. 4c). Endocytosis, an energy-dependent uptake, of nanoparticles could be effectively inhibited by lowering the culture temperature.[39,40] With TAM observation, we have found that the average number of NDs in each cell is greatly reduced to less than 20% of the control group (Fig. 4d). Similarly, the respiration inhibitor sodium azide[39,41] also caused similar reduction of the cell uptake of NDs (Fig. 4e). Cells with hypertonic treatment using sucrose[39,42] reduced the cell uptake to 20% of the normal conditions as well (Fig. 4f). All these experiments supported the endocytosis mechanism of the cell uptake, in accordance with previous research.[43,44]

In summary, we present transient absorption as a contrast source to detect raw NDs in live cells for the first time. These label-free NDs can be transported into cells through endocytosis, allowing whole processes to be monitored with a high-speed TAM system. Because this technique is highly sensitive, intrinsically 3D, yields minimal photodamage, and has low autofluorescence, transient absorption is a unique and potentially powerful imaging platform to study biological applications of raw NDs without labeling.

Acknowledgements

The authors thank Prof. Jianzhong Xi, Prof. Yujie Sun, Dr Liang Zhao and Mr Xiaopeng Ma for their help. This work was supported by the Ministry of Science and Technology of China (Grant no. 2011CB809106), the National Science Foundation of China (Grant no. 91913011, 21222501), and the Fok Ying Tung Education Foundation. A. M. S. was supported by the Whitaker International Biomedical Engineering Fellowship.

Notes and references

1 R. Y. Tsien, *Annu. Rev. Biochem.*, 1998, **67**, 509.
2 X. Michalet, F. F. Pinaud, L. A. Bentolila, J. M. Tsay, S. Doose, J. J. Li, G. Sundaresan, A. M. Wu, S. S. Gambhir and S. Weiss, *Science*, 2005, **307**, 538.
3 H. Wang, T. B. Huff, D. A. Zweifel, W. He, P. S. Low, A. Wei and J. X. Cheng, *Proc. Natl. Acad. Sci. U. S. A.*, 2005, **102**, 15752.
4 N. J. Durr, T. Larson, D. K. Smith, B. A. Korgel, K. Sokolov and A. Ben-Yakar, *Nano Lett.*, 2007, **7**, 941.
5 A. Albanese, P. S. Tang and W. C. W. Chan, *Annu. Rev. Biomed. Eng.*, 2012, **14**, 1.
6 V. Bagalkot, L. Zhang, E. Levy-Bissenbaum, S. Jon, P. W. Kantoff, R. Langer and O. C. Farokhzad, *Nano Lett.*, 2007, **7**, 3065.
7 Z. Liu, M. Winters, M. Holodniy and H. Dai, *Angew. Chem., Int. Ed.*, 2007, **46**, 2023.
8 C. C. Chen, Y. P. Lin, C. W. Wang, H. C. Tzeng, C. H. Wu, Y. C. Chen, C. P. Chen, L. C. Chen and Y. C. Wu, *J. Am. Chem. Soc.*, 2006, **128**, 3709.
9 A. C. Bonoiu, S. D. Mahajan, H. Ding, I. Roy, K. T. Yong, R. Kumar, R. Hu, E. J. Bergey, S. A. Schwartz and P. N. Prasad, *Proc. Natl. Acad. Sci. U. S. A.*, 2009, **106**, 5546.
10 X. Sun, Z. Liu, K. Welsher, J. T. Robinson, A. Goodwin, S. Zaric and H. Dai, *Nano Res.*, 2008, **1**, 203.
11 Z. Liu, J. T. Robinson, X. Sun and H. Dai, *J. Am. Chem. Soc.*, 2008, **130**, 10876.
12 Y. Wang, Z. Li, D. Hu, C. T. Lin, J. Li and Y. Lin, *J. Am. Chem. Soc.*, 2010, **132**, 9274.
13 N. W. S. Kam, M. O'Connell, J. A. Wisdom and H. Dai, *Proc. Natl. Acad. Sci. U. S. A.*, 2005, **102**, 11600.
14 D. Ho, *ACS Nano*, 2009, **3**, 3825.
15 H. Huang, E. Pierstorff, E. Osawa and D. Ho, *Nano Lett.*, 2007, **7**, 3305.
16 L. M. Manus, D. J. Mastarone, E. A. Waters, X. Q. Zhang, E. A. Schultz-Sikma, K. W. MacRenaris, D. Ho and T. J. Meade, *Nano Lett.*, 2010, **10**, 484.
17 V. N. Mochalin, O. Shenderova, D. Ho and Y. Gogotsi, *Nat. Nanotechnol.*, 2012, **7**, 11.
18 V. V. Danilenko, *Phys. Solid State*, 2004, **46**, 595.
19 J. P. Boudou, P. A. Curmi, F. Jelezko, J. Wrachtrup, P. Aubert, M. Sennour, G. Balasubramania, R. Reuter, A. Thorel and E. Gaffet, *Nanotechnology*, 2009, **20**, 235602.
20 M. Fremklach, W. Howard, D. Huang, J. Yuan, K. E. Spear and R. Koba, *Appl. Phys. Lett.*, 1991, **59**, 546.
21 W. W. Zheng, Y. H. Hsieh, Y. C. Chiu, S. J. Cai, C. L. Cheng and C. P. Cheng, *J. Mater. Chem.*, 2009, **19**, 8432.
22 V. N. Mochalin, I. Neitzel, B. J. M. Etzold, A. Peterson, G. Palmese and Y. Gogotsi, *ACS Nano*, 2011, **5**, 7494.
23 A. Krueger and T. Boedeker, *Diamond Relat. Mater.*, 2008, **17**, 1367.
24 X. Q. Zhang, M. Chen, R. Lam, X. Xu, E. Osawa and D. Ho, *ACS Nano*, 2009, **3**, 2609.
25 Y. R. Chang, H. Y. Lee, K. Chen, C. C. Chang, D. S. Tsai, C. C. Fu, T. S. Lim, Y. K. Tzeng, C. Y. Fang, C. C. Han, H. C. Chang and W. Fann, *Nat. Nanotechnol.*, 2008, **3**, 284.
26 S. J. Yu, M. W. Kang, H. C. Chang, K. M. Chen and Y. C. Yu, *J. Am. Chem. Soc.*, 2005, **127**, 17604.
27 D. Fu, T. Ye, T. E. Matthews, B. J. Chen, G. Yurtserver and W. S. Warren, *Opt. Lett.*, 2007, **32**, 2641.
28 T. Ye, D. Fu and W. S. Warren, *Photochem. Photobiol.*, 2009, **85**, 631.
29 L. Tong, Y. Liu, B. D. Dolash, Y. Jung, M. N. Slipchenko, D. E. Bergstrom and J. X. Cheng, *Nat. Nanotechnol.*, 2012, **7**, 56.
30 K. K. Liu, C. C. Wang, C. L. Cheng and J. Chao, *Biomaterials*, 2009, **30**, 4249.
31 C. W. Freudiger, W. Min, B. G. Saar, S. Lu, G. R. Holtom, C. He, J. C. Tsai, J. X. Kang and X. S. Xie, *Science*, 2008, **322**, 1857.

32 W. Min, S. Lu, S. Chong, R. Roy, G. R. Holtom and X. S. Xie, *Nature*, 2009, **461**, 1105.
33 C. N. Lincoln, E. Fitzpatrick and J. J. v. Thor, *Phys. Chem. Chem. Phys.*, 2012, **14**, 15752.
34 R. Sander, V. Herrmann and R. Menzel, *J. Chem. Phys.*, 1996, **104**, 4390.
35 L. Nagli, M. Gaft, Y. Fleger and M. Rosenbluh, *Opt. Mater.*, 2008, **30**, 1747.
36 Y. J. Tian, J. Zuo, L. Y. Zhang, Z. W. Li, S. Q. Gao and G. H. Lu, *Appl. Phys. B: Lasers Opt.*, 2007, **87**, 727.
37 S. Fisher-Parton, R. M. Parton, P. C. Hickey, J. Dijksterhuis, H. A. Atkinson and N. D. Read, *J. Microsc.*, 2000, **198**, 246.
38 M. A. Penalva, *Fungal Genet. Biol.*, 2005, **42**, 963.
39 S. C. Silverstein, R. M. Steinman and Z. A. Cohn, *Annu. Rev. Biochem.*, 1977, **46**, 669.
40 R. M. Steinman, J. M. Silver and Z. A. Cohn, *J. Cell Biol.*, 1974, **63**, 949.
41 P. Scarmato, G. Durand, J. Agneray and J. Feger, *Biol. Cell*, 1986, **56**, 255.
42 J. E. Heuser and R. G. W. Anderson, *J. Cell Biol.*, 1989, **108**, 389.
43 O. Faklaris, V. Joshi, T. Irinopoulou, P. Tauc, M. Sennour, H. Girard, C. Gesset, J. C. Arnault, T. Thorel, J. P. Boudou, P. A. Curmi and F. Treussart, *ACS Nano*, 2009, **3**, 3955.
44 B. Zhang, Y. Li, C. Y. Fang, C. C. Chang, C. S. Chen, Y. Y. Chen and H. C. Chang, *Small*, 2009, **5**, 2716.

Supporting Information

Optical Imaging of the Non-fluorescent Nanodiamonds in Live Cells Using Transient Absorption Microscopy

Tao Chen,[+][a] Feng Lu,[+][b] Aaron M. Streets,[a] Peng Fei,[a] Junmin Quan[b] and Yanyi Huang[a]*

[a] *Biodynamic Optical Imaging Center (BIOPIC), and College of Engineering, Peking University, Beijing, China. Fax: +86-010-62758323; Tel: +86-010-62744058; E-mail: yanyi@pku.edu.cn*
[b] *School of Chemical Biology and Biotechnology, Peking University Shenzhen Graduate School, Shenzhen, China.*
[+] These authors contributed equally

Methods and Materials

Preparation of the nanodiamonds (NDs)

The raw, detonated NDs (NanoCarbon Institute, Japan) were acquired as colloidal particles and then dispersed in deionized water. The raw ND colloid was carboxylated in strong oxidizing conditions as previously reported.[30] Briefly, the colloid was treated in acid mixture of 68% HNO3 : 98% H_2SO_4 (1:3 in volumn) in ultrasonic bath for 24 h, followed by stirring in 0.1 M NaOH at 90 °C for 2 h. After high-speed centrifugation, an additional stirring was performed in 0.1M HCl aqueous solution at 90 °C for 2 h, and finally sent for high-speed centrifugation. The pellet was resuspended in deionized water and precipitated again by high-speed centrifugation. This procedure was repeated three times to remove excessive HCl and impurities. A minute portion of the aqueous suspension was dispensed on a silicon wafer and characterized with scanning electron microscopy.

Cell culture

The NIH 3T3 fibroblast cells were maintained in Dulbecco's modified Eagle medium (DMEM) complete media containing 10% new born calf serum (NBCS) and 1% penicillin-streptomycin mix. Cells were plated onto 6-well plates at a concentration of 10^5/cm2 and cultured in a humidified incubator at 37°C and 5% CO_2 atmosphere.

Transient absorption microscope (TAM)

The TAM was constructed from a modified two-photon scanning microscope system. Light source for TAM is a pump source integrated optical parametric oscillator, also known as one-box OPO (picoEmerald, Berlin, Germany). This one-box OPO can simultaneously provide two spatially and temporally overlapped pulse trains, with a repetition rate of 80MHz. The wavelength of one beam is 1064 nm (the pump beam in TAM), and the other is tunable between 720-990nm (the probe beam in TAM). Pulse duration is 8ps for the 1064nm beam and 6ps for the tunable laser. The two beams are sent into an inverted multiphoton microscope (IX81/FV1000, Olympus, Japan). Intensity of the 1064nm beam

is modulated with an electro-optic modulator (EO-AM-NR-C2, Thorlabs, USA) at 9.81 MHz. The two beams are co-aligned and focused by a 60X water immersion objective (UPLSAPO 60XW, Olympus, Japan), where they scan over the sample through galvo mirrors in the scanning unit. After transmitting through the sample, the probe beam is collected by a water immersion condenser (N.A. 0.9, Olympus, Japan), then focused to a large area photodiode (FDS1010, Thorlabs, USA). The photo-electric signal was sent into a lock-in amplifier (designed by Dr. Brian Saar). After demodulation, the amplified signal was sent into an A/D converter, and then used to reconstruct images. Stimulated Raman scattering signal of paraffin's CH2 stretching mode (2845 cm^{-1}) was acquired to characterize the system response and reveal the correlation between the two pulse trains.

Raman Spectra Measurement

Spontaneous Raman spectrum was acquired with a confocal microscopic Raman spectrometer (HR800, HORIBA, Japan), excited with a 532nm laser. ND suspension was spun on a slide and dried before spectrum collection.

Absorption Spectrum

Absorption spectrum was acquired with a UV-VIS spectrometer (UV2450, SHIMADZU, Japan). Spectra of aqueous solution were acquired ten times for noise suppresion.

Laser Power Tolerance

IR lasers ranging from 810nm to 1064nm were used for TAM imaging. Cells don't absorb much light in this wavelength region. Cells were irradiated with both pump and probe beams. Pump beam was set at its maximum power, 350mW. Probe beam power was changed from 400mW to 700mW. These powers indicate the output from the laser head. Throughput from the laser head to the sample was measured to be 6.7% for the pump and 19.1% for the probe beam. Irradiation time for each power combination is 220 s. Results were recorded and shown in Fig. S2-S6.

Cell uptake experiment

The ND suspension was sonicated for over 8 h and mixed with culture medium. This ND-containing mixture was then used to replace the normal medium to culture 3T3 cells for 8 h. Extracellular NDs were washed away by PBS before imaging. Transmission images and transient absorption images were acquired sequentially in the same field of view. To validate the uptake mechanism, cells were stained with the amphiphilic fluorescent dye FM4-64 (Invitrogen). The lipophilic tail of FM4-64 can insert into cellular phospholipid membrane, stain the membrane specifically and firmly [1]. Simultaneously, ND-containing medium was added to the stained cells and cultured for another 4 h before imaging. Fluorescence and transient absorption images were acquired sequentially.

TAM intrinsically has 3D imaging capability. Fig. S7 showed the distribution of NDs in 3T3 cell when changing focal plane.

To monitor the dynamics of cell uptake, we cultured the cells in petri dishes with an on-stage incubator (Chamlide TC-A, LCI, Korean). Image acquisition started right after the

introduction of NDs. Images were acquired in three dimensions with 1 um steps in z direction, 7 sections for each stack. It took 17 s to finish a stack and ~ 1 h to finish the 3D time-lapse observation. The same batch of cells was cultured under the different conditions for test cell uptake. For each condition, cells were cultured for 3 h, and then 6 random locations in the Petri dish were picked for imaging. We also adjusted the experimental schedule to ensure that the cells were treated for the same amount of time under different conditions before the image acquisition. Three-dimensional images using both transmission and transient absorption were taken for each field-of-view. The number of particles taken up by the cells was counted in each image using FIJI [2]. For each field of view, total intensity in the whole volume was calculated, and divided by cell numbers. Particles taken per cell were used to compare uptake ability under each condition.

MTT Assay

MTT assay [3] was applied to cells to measure the viability of cells treated with NDs. Cells were co-cultured with NDs for 8 hours before the experiments. The assay was carried out under two conditions, with serum and without NBCS. For both conditions, NDs concentrations in ratio of 1:2:3 were applied. For each concentration each condition, 6~7 groups were set. This entire assay was repeated three times.

Signal Confirmation

Stimulated Emission (SE) is the process to induce fluorescence with pump-probe scheme in non-fluorescent species. To rule it out, we checked the phase of our signal, as illustrated in Fig. S10.

For clarity, we use phase of SRS as reference. The SRS we detected is the loss of pump. Transient absorption here showed the same phase with SRS. However, for SE, it has the opposite phase compared with SRS. In Fig3 C, we can see SRS and TA were both brighter than background, indicating they have the same phase. If not, those spots representing NDs should be darker than background.

References:

[1] Cochilla, A. J.; Angleson, J. K.; Betz, W. *Annu. Rev. Neurosci.* **1999**, *22*, 1-10.
[2] Schindelin, J.; Arganda-Carras, I.; Frise, E.; Kaynig, V.; Longair, M.; Pietzsch, T.; Preibisch, S.; Rueden, C.; Saalfeld, S.; Schmid, B.; Tinevez, J. Y.; White, D. J.; Hartenstein, V.; Eliceiri, K.; Tomancak, P.; Cardona, A. *Nat. Methods*, **2012**, *9*, 676-682.
[3] Mosmann, T. *J. Immunol. Methods,* **1983**, *65 (1-2)*, 55-63.

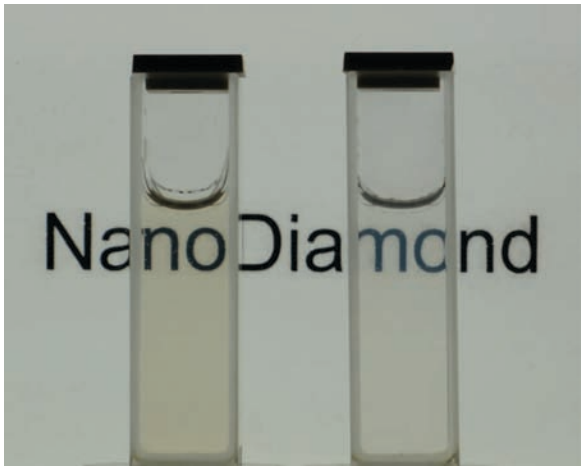

Fig. S1. A photograph of raw (left) and carboxylated (right) NDs in cuvettes.

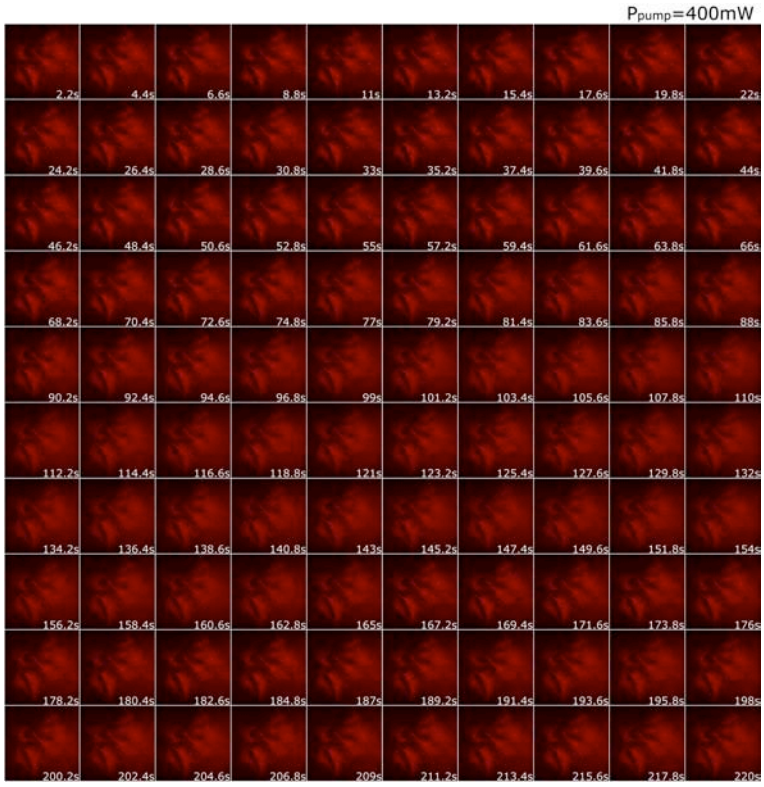

Fig. S2. Selected time-lapse TAM images of raw NDs in the live fibroblast cells. The power of the pump beam was set to 400 mW.

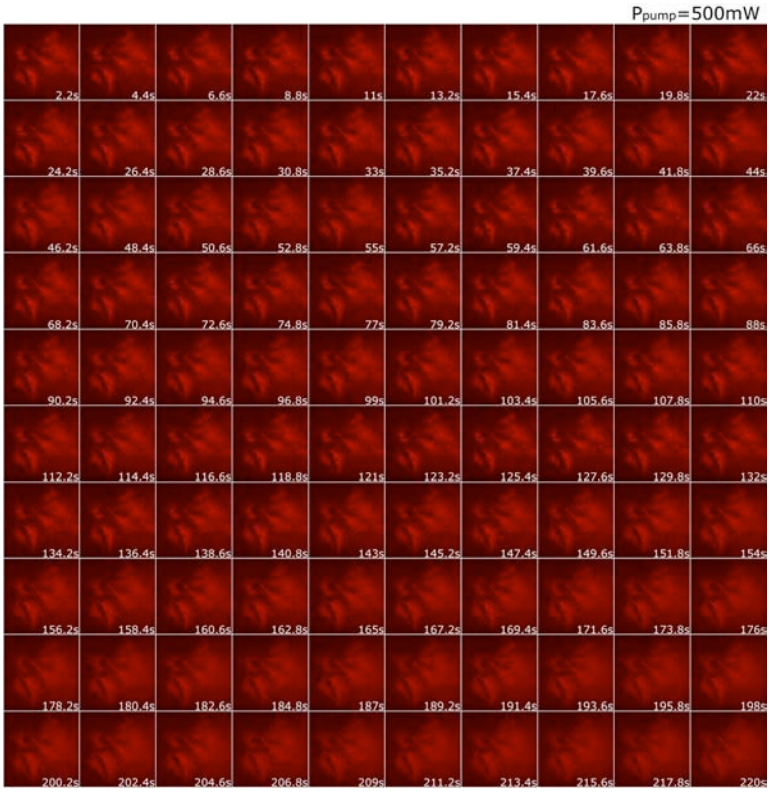

Fig. S3. Selected time-lapse TAM images of raw NDs in the live fibroblast cells. The power of the pump beam was set to 500 mW.

Fig. S4. Selected time-lapse TAM images of raw NDs in the live fibroblast cells. The power of the pump beam was set to 600 mW.

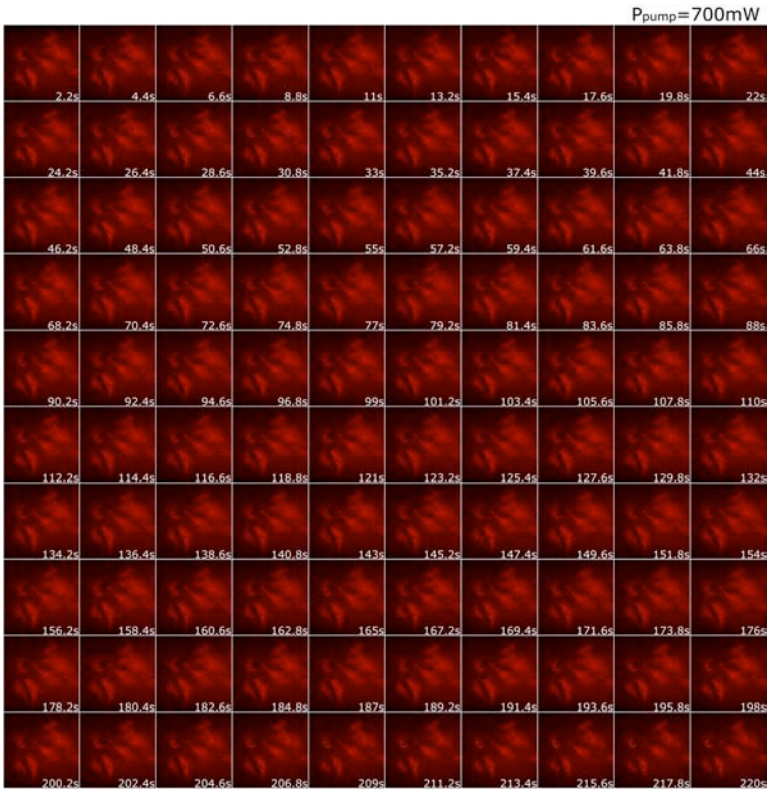

Fig. S5. Selected time-lapse TAM images of raw NDs in the live fibroblast cells. The power of the pump beam was set to 700 mW.

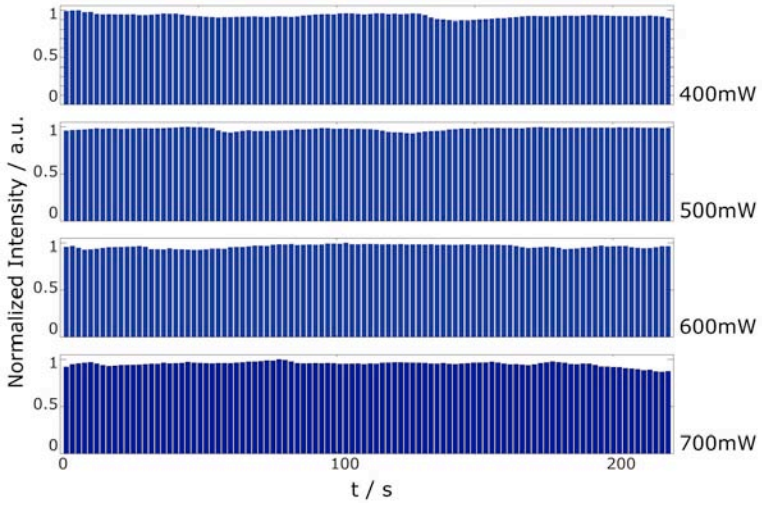

Fig. S6. The normalized TA intensity of the TA images during the continuous imaging acquired with various pump intensity (also check Fig. S2-S5).

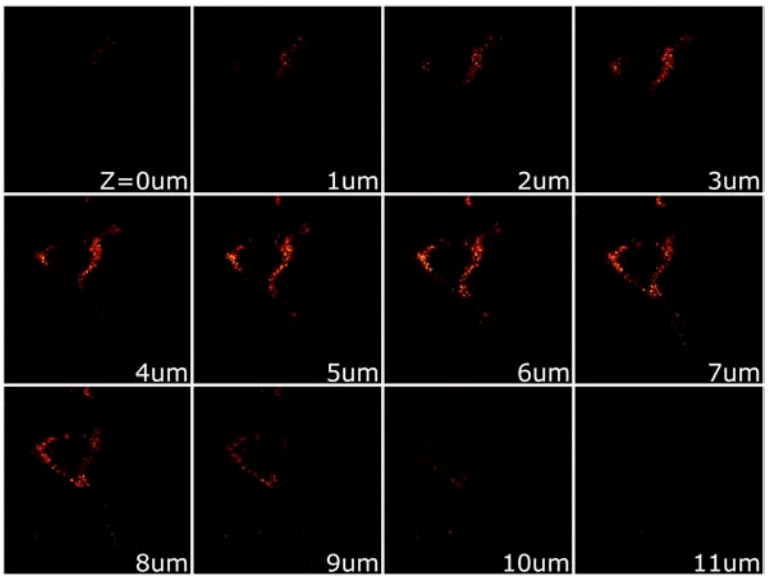

Fig. S7. A stack of TAM images taken at the different focal plane, representing the intrinsic 3D sectioning of the TAM.

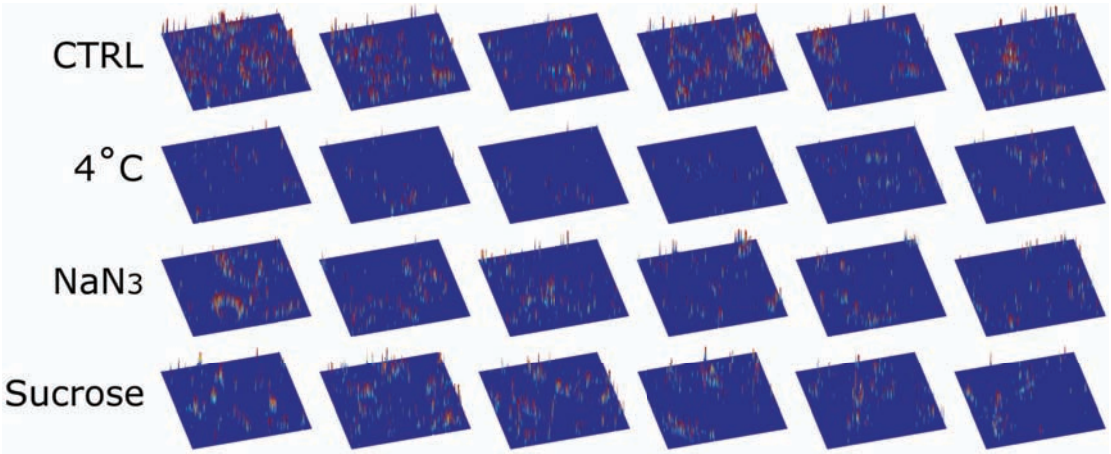

Fig. S8. Comparison of NDs in cells under different culture conditions. Results of six experiments were shown. Variation between different experiments is evident. Meanwhile, in all experiements changing the culture conditions lead to reduction of NDs uptake.

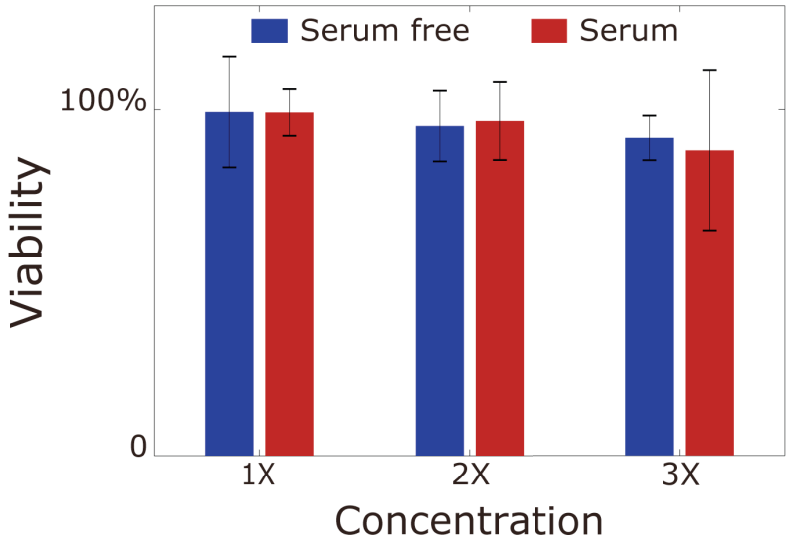

Fig. S9. MTT assay result for 3T3 cells co-cultured with NDs for 8 hours. The variation originated from cell proliferation.

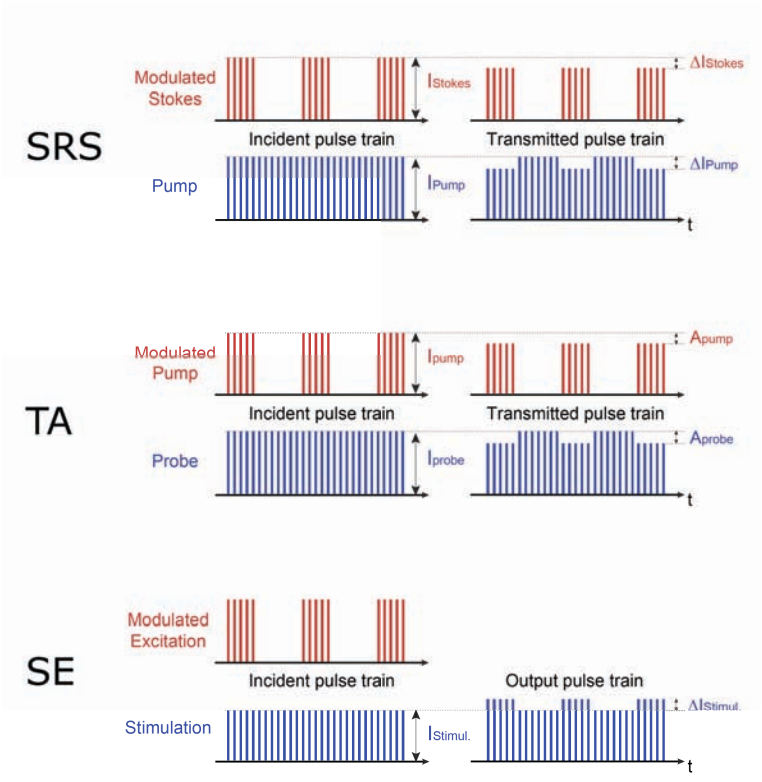

Fig. S10. Phase Comparison between stimulated Raman scattering (SRS), transient absorption (TA), and stimulated emission (SE). SRS and TA show the same phase, meanwhile SE shows the opposite phase.